

# **Reservoir Engineering: An Introduction and Application to Rico, Colorado**

Geothermal Energy – MNGN598  
Dr. Masami Nakagawa

Due 7 May 2009

**By**

**Jeff Reindl  
Han Shen  
Terry Bisiar**

## Table of Contents

1.0 Rico Location and History.....	4
2.0 Reservoir Engineering Background.....	5
3.0 Elements of Geothermal Reservoirs.....	5
3.1 General Geology of Geothermal Reservoirs.....	5
3.2 Rock Properties.....	5
3.2.1 Porosity.....	5
3.2.2 Permeability.....	6
3.3 Well Logging and Geophysical Evaluation.....	7
3.4 Geothermal Fluid Properties.....	7
3.4.1 Geochemical Analysis.....	8
3.4.2 Composition of Geothermal Fluids.....	8
3.4.3 Sources of Dissolved Solids.....	8
3.4.4 Specific Physical and Chemical Properties of Geothermal Reservoir Fluids.....	9
3.4.4.1 PH.....	9
3.4.4.2 Bubble Point Pressure.....	9
3.4.4.3 Formation Volume Factor of Geothermal Water.....	9
3.4.4.4 Density.....	10
3.4.4.5 Solubility of Gas in Geothermal Fluids.....	11
3.4.4.6 Coefficient of Isothermal Compressibility in Water.....	12
3.4.4.7 Viscosity.....	12
3.4.4.8 Enthalpy.....	13
3.5 Implications of Changing Fluid Properties.....	13
3.6 Heat Flow in Reservoirs.....	14
4.0 Reservoir Calculations.....	15
4.1 Volume.....	15
4.2 Flow Rate Calculation.....	16
5.0 Reservoir Types.....	17
6.0 Fracture of Rock.....	16
7.0 Reservoir Recharge and Injection Processes.....	19
8.0 Case History.....	19
9.0 Rico Reservoir Model.....	19
9.1 Geological Setting.....	19
9.2 Possible Formation Top Determination.....	21
9.3 Well Log Data.....	21
9.4 Volumetric Calculations.....	23
9.5 Flow Rates and Associated Calculations.....	24
9.6 Recharge Model.....	25
9.7 Re-injection Possibilities.....	26
9.8 Case Study.....	27
9.9 Reservoir Characterization.....	27
10.0 Future.....	27

11.0	References.....	28
12.0	Appendix A.....	30
13.0	Appendix B.....	34

## List of Figures

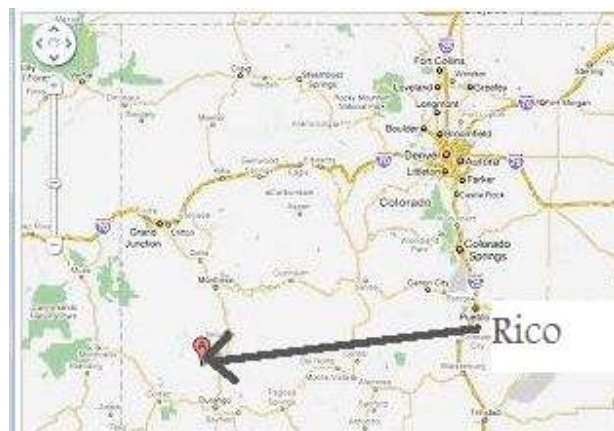
<b>Figure 1:</b>	Geographical location of Rico, CO (google/maps, 2009).....	4
<b>Figure 2:</b>	Pressure-temperature curve of pure substance(McCain, 1990).....	9
<b>Figure 3:</b>	Formation Volume Factor of Water (McCain, 1990).....	10
<b>Figure 4:</b>	Density of water at different pressures and temperatures (Chaplin, 2009).....	11
<b>Figure 5:</b>	Solubility Curve related to pressure (McCain, 1990) .....	12
<b>Figure 6:</b>	Viscosity of brine water (McCain, 1990).....	13
<b>Figure 7:</b>	Poss. shifts in fluid state if reservoir temperature and pressure are changed...13	
<b>Figure 8:</b>	Depth relationship with heat transfer mechanism. From Dipippo (1997).....	15
<b>Figure 9:</b>	Schematic of conduction and convection within a reservoir.....	15
<b>Figure 10:</b>	General radial flow into wellbore (Dipippo, 2007).....	17
<b>Figure 11:</b>	Stratigraphy of possible Rico reservoir formation (UGS, 2007).....	20
<b>Figure 12:</b>	Typical effects of tectonic events on crust (Dipippo, 2007).....	20
<b>Figure 13:</b>	Log sections and well locations near Rico (COGCC, 2009).....	22
<b>Figure 14:</b>	Inputs for Volumetric Monte Carlo Simulation.....	23
<b>Figure 15:</b>	Volumetric output using a Monte Carlo Simulation.....	23
<b>Figure 16:</b>	Inputs for flow rate calculation using Monte Carlo Simulation.....	24
<b>Figure 17:</b>	Flow rate output using a Monte Carlo Simulation.....	25
<b>Figure 18:</b>	Hypothesized catchment Basin (Tecplot and Google Maps).....	26
<b>Figure 19:</b>	Schematic of possible Rico geothermal reservoir.....	27

## List of Tables

<b>Table 1:</b>	Typical geothermal lithologies and corresponding porosity and permeabilities (Graves, 2008; Geosociety, 2008).....	6
<b>Table 2:</b>	Typical thermal conductivities of common lithologies. From Dipippo(2007).	14
<b>Table 3:</b>	Flow rates from springs near Rico (Pearl, 1979).....	24

## 1.0 Rico Location and History

The town of Rico, Colorado is located at  $37^{\circ}41'32''\text{N}$   $108^{\circ}1'51''\text{W}$ , which lies in the east edge of Delores County shown in **Figure 1**. It is just over 80 miles from Durango and about 25 miles from nearby Telluride. Rico is most commonly known for its rich mining history, which dates back to the late 1800s and continues on a limited basis today. It is believed that geothermal fluids influenced many of the ore deposits over the region. Numerous surface geothermal springs indicate that a larger scale hydrothermal source may exist in the subsurface. This resource may have the potential for possible district-usage applications and possible use in electricity generation.



**Figure 8:** Geographical location of Rico,CO (google/maps, 2009)

## 2.0 Reservoir Engineering Background

Reservoir engineering was originally developed as a discipline in the oil and gas industry around the 1930s and became much more important during the 1960s and 1970s with the availability of computers to run model data (Whiting and Ramey, 1969). It is a “joint application of geological and engineering data” which allows for the successful development of reservoir models (Craft and Hawkins, 1991). Kjaran and Eliasson (1983) even suggest that reservoir engineers are more artists than scientists. Reservoir engineers must make use of a variety of disciplines such as geology, chemistry, thermodynamics, and fluid mechanics in order to successfully develop a viable model. It is this variety and the lack of quantitative data that drive reservoir engineers to be creative and imaginative in their model construction.

Geothermal reservoirs should be considered a resource. As with oil and gas resources, there is risk and uncertainty in accurately locating and producing the resource. In order to reduce the potential risk, previous research done on regional geology, associated geophysical and well logging, as well as geochemical data should be analyzed. This type of a history match will help better provide better understanding of where to potentially use geophysical techniques or drill an exploratory well. Due to the lack of geothermal

development in many regions of the United States, little data of this sort exists. However, there is an abundance of geology and well log data pertaining to oil and gas exploration. Most states require submission of well logs and therefore it is available to the public.

After gathering data on regional geology and well log data, the reservoir should be characterized by its rock properties, physical properties, geochemical results, and geologic setting. The analysis of these properties will drive exploration strategies, drilling procedures, production and volumetric calculations, and production infrastructure. Reservoir evaluation is a major factor in economic evaluation and feasibility of the project.

The main goal of this project will be to provide a simplified approach to reservoir evaluation and engineering principles. Building on these ideas, several conceptual models will be built as a starting place for a more quantitative analysis. Finally, using the available resources, the Rico geothermal resource will be evaluated and recommendations will be made.

### **3.0 Elements of Geothermal Resources**

All types of geothermal reservoirs have certain common characteristics which define them as potential sustainable resources. Dippio(1998) suggests five aspects which make a geothermal reservoir commercially viable for development.

- (1) Heat source
- (2) Permeability
- (3) Volume
- (4) Seal
- (5) Recharge Mechanism

### **3.1 General Geology of Geothermal Reservoirs**

All geothermal reservoirs will have the same general architecture. The reservoir will contain a fluid source, which typically is a highly porous and permeable rock, and sealing mechanisms. Sealing mechanisms will prevent migration of geothermal fluid to the surface due to an impermeable barrier. In the case of a geothermal system, a heat source must be present such as an igneous intrusion or shallow magma.

### **3.2 Rock Properties**

Several of the most important factors for a viable geothermal reservoir are related to the reservoir rock properties. Porosity, permeability, and rock compressibility are the three most important rock properties.

#### **3.2.1 Porosity**

When determining the viability of a geothermal resource, its volumetric potential must be investigated. A reservoir's porosity is critical to volumetric calculations, which will be presented later in this paper. Porosity can simply be defined as the ratio between the volume of total void space in the rock matrix and the total volume of the rock.

$$\Phi = V_{\text{pore}}/V_{\text{bulk}} = (V_{\text{bulk}} - V_{\text{grain}})/V_{\text{bulk}}$$

Theoretically, porosity is defined in this manner. However, in reality, an effective permeability exists. This type of porosity accounts for the notion that not all of the pore space is interconnected and that interstitial liquid exists in the reservoir. Interstitial liquid remains bound to the surface of the rock grains and cannot be released (Karjan and Elisason, 1982; Craig, 1973). Karjan and Eliasson (1982) define effective porosity as follows.

$$\Phi_{\text{effective}} = \Phi * \text{Fluid free to move} / \text{Fluid in storage}$$

Effective porosity is much smaller than theoretical porosity. Unfortunately, it is very difficult to directly measure this property. It can be measured with some accuracy by crushing a core sample. While this property is difficult to measure, it still should be considered during the analysis, as effective porosity will represent the volume of fluid, which can actually be utilized. For simplicity, however, this paper will treat effective and theoretical porosity as the same.

Porosity can be subject to diagenetic processes. Primary porosity is the porosity of a rock at the time of deposition. Secondary porosity, which is typically significantly lower than primary porosity, is a result of grain compaction caused by large overburden pressures or cementation caused by chemical processes, which occurred after burial. In some cases, typically in limestone, secondary processes may increase porosity through dissolution and formation of vugs. Porosity is a function of grain sorting.. **Table 1** summarizes typical porosities (and permeabilities) for common rock lithologies.

<b>Lithology</b>	<b>Porosity (%)</b>	<b>Permeability (D)</b>
Sandstone	< 40	$5*10^{-4}$ - 3.0
Tight Sandstone	8 - 10	$5*10^{-4}$ - 3.0
Limestone	5 - 25	$2*10^{-4}$ - $4.5*10^{-2}$
Rhyolite	30 - 60	N/A

**Table 1:** Typical geothermal lithologies and corresponding porosity and permeabilities (Graves, 2008; Geosociety, 2008)

Porosity can be measured in several different ways. Core analysis techniques can be used to make very accurate measurements. Various well logs can estimate porosity. Well logs that can be used include resistivity, neutron porosity, density, and sonic.

### 3.2.1 Permeability

The permeability of a reservoir rock is crucial to correctly evaluating a geothermal resource. Schlumberger (2009) describes permeability as the ability of rock to transmit fluids through porous media. Permeability values can be used in conjunction with Darcy's Law to determine flow rates of a reservoir. Permeability is defined as the following.

$$K = -\mu * Q * L / A * \Delta P$$

Permeability has units of Darcys (or milliDarcys), which is a unit of length squared. The above equation for permeability is for single phase, slug flow fluid movement. The equation can be modified to include effects of multi-phase flow as well as directional permeability.

### 3.3 Well Logging and Geophysical Evaluation

Often the best starting point for geothermal exploration is through the use of geophysical techniques such as gravity and magnetics. These methods help make predictions about lithology, faulting, and fluid movement in and out of the reservoir. If adequate funding is available, 2-D or 3-D seismic can be run over a region. This provides a very good data set for interpretation of faulting and placement of wells.

Common well logging techniques used in the geothermal industry include temperature gradient logs, gamma ray, bulk density, neutron porosity, resistivity, and sonic logs. Logging techniques help determine reservoir rock properties and in situ fluid properties, which are required for reservoir calculations.

Temperature gradient logs help determine temperatures from bottom hole to the surface. High bottom hole temperatures provide the most potential when evaluating a resource. In most cases, geothermal reservoirs will exhibit low gamma ray readings, which indicate "clean" (little mixing with clay) sandstone or limestone. However, some reservoirs which are igneous may show very high gamma ray responses, such as Rhyolite (in Idaho). Bulk density logs yield porosity after being converted using a specified formation density (2.65gm/cc for sandstone and 2.71 gm/cc for limestone). Calculation is typically done by the logging service company. Neutron porosity provides an alternative measurement of porosity. By plotting neutron porosity and density porosity (from bulk density log) on the same graph, zones which may contain large amounts of gas can be determined by a characteristic crossover in logs. This is known as the gas effect. Resistivity logs provide information about the in situ fluid type. Low resistivity readings indicate the presence of a highly conductive fluid such as a geo-fluid. Water saturation can be determined using Archie's equation as well. Sonic logs provide indications of lithology and porosity. For further details of basic well log analysis please refer to *Basic Well Log Analysis* by Asquith and Krygowski (2004).

### 3.4 Geothermal Reservoir Fluid Properties

Over the course of history of the oil and gas industry, there has been one major commonality to nearly every reservoir. This common element is production of water. There has been quite a bit of research done on oilfield waters and particularly the properties that make them corrosive. In the context of geothermal fluids, there have been numerous studies done of geochemical properties of geothermal fluids. These geochemical properties have been used mainly for exploration purposes. The attempt will be to use oilfield water properties as a backbone for the understanding of geothermal fluid properties.

### **3.4.1 Geochemical Analysis**

In most cases, before a well is ever drilled in a geothermal region, geochemical observations will be taken. This is an inexpensive and relatively simple method to obtain basic reservoir information. Surface features such as springs or hydrothermally altered surface rock may be analyzed. Geochemical techniques such as geothermometry can help determine possible reservoir temperatures. In addition, geochemical analysis of dissolved solids can show the possible types of reservoir rock and whether a reservoir is fluid or vapor dominated. Finally, Geochemical analysis can help determine the origin of the recharge fluid to the reservoir (DiPeppo,1997). Conceptual recharge models can be developed from this data.

### **3.4.2 Composition of Geothermal Fluids**

Produced formation geothermal fluids, in most cases, will contain amounts of dissolved solids. These dissolved solids are ionic in nature. Most oilfield waters contain primarily large concentrations of Sodium Chloride (NaCl) (McCain, 1990). Typical ranges for total dissolved solids (TDS) in geothermal fluids fall within the same range as oilfield waters, which are from about 200 ppm to saturation ( can exceed 300,000 ppm). It is common, in the western United States, for geothermal fluids to contain between 6,000 to 10,000 mg/l (TDS). However, in parts of the Imperial Valley in California, TDS can reach 300,000 mg/l. Typical constituents that contribute to the TDS include  $\text{SiO}_2$ ,  $\text{Ca}^{2+}$ ,  $\text{Mg}^{2+}$ ,  $\text{Na}^+$ ,  $\text{K}^+$ ,  $\text{Li}^+$ ,  $\text{HCO}^-$ ,  $\text{SO}_4^{2-}$ ,  $\text{Cl}^-$ ,  $\text{F}^-$ , B, As,  $\text{HCO}_3^-$ , and  $\text{SO}_4^{2-}$ . Trace amounts of up to 40 other ions can occur in some oilfield waters and likely in geothermal fluids. The traditional manner to present the distribution of ions is in the form of a Stiff Diagram.

### **3.4.3 Sources of Dissolved Solids**

The source of dissolved solids lie within the formation where the fluid is generated. Ionic components of the fluid may originate from biologic processes, adsorption and base exchange with clay materials, dissolution of mineral salts, Ca and Mg exchange during dolomitization, salt sieving by shales, chemical precipitation, and chemical reactions with the reservoir sediments (McCain, 1990).



### 3.4.4 Specific Physical and Chemical Properties of Geothermal Reservoir Fluids

#### 3.4.4.1 pH

The pH of produced waters influences equilibrium reactions that take place continuously in solution. Changes in pH upon evolution can change the chemical characteristics of the fluids. Most geothermal waters range from 5.5 to 8.5 in pH. If a pH changes, reservoir pore space and fracture space may become plugged by precipitants and this can cause a decrease in production.

#### 3.4.4.2 Bubble Point Pressure

The bubble point pressure of a geothermal fluid is defined as the pressure at which dissolved gas may evolve from the fluid. If a pressure is above the bubble point pressure, then all of the fluid will remain in the liquid phase. This parameter governs many of the variables that are needed for reservoir calculations. Note that the bubble point pressure is also known as the vapor pressure. **Figure 2** illustrates a typical pressure temperature curve for a pure substance such as water. The bubble point pressure is defined by the vapor-pressure line on the curve.

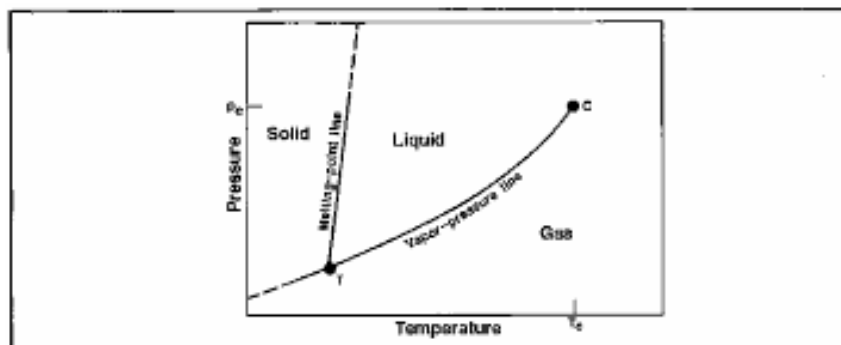


Figure 9: Pressure-temperature curve of pure substance(McCain, 1990)

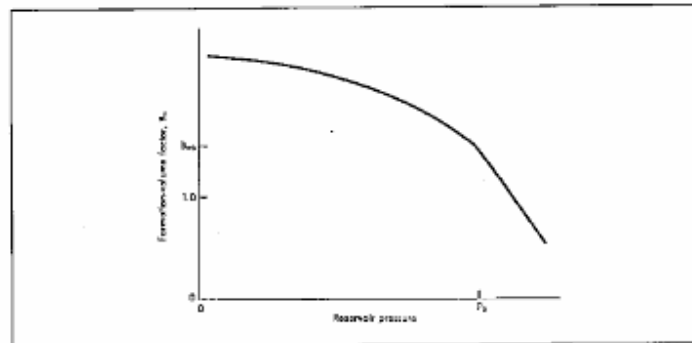
#### 3.4.4.3 Formation Volume Factor of Geothermal Water

The formation volume factor of water,  $B_w$ , has been defined by McCain (1990) as the representation of the change in volume of fluid as it is transported from the reservoir to the surface. Typical units of  $B_w$  are in reservoir bbl/STB or in this case  $\text{ft}^3/\text{SCF}$ . There are three effects that influence  $B_w$ :

1. evolution of dissolved gas from geo-fluids as pressure decreases – most influential
2. expansion of fluids as pressure is reduced
3. contraction of geo-fluids as temperature decreases

Typical  $B_w$  are about 1.06 res bbl/STB or 1.06  $\text{ft}^3/\text{SCF}$ .  $B_w$  is a dynamic and changing property. **Figure 3** illustrates its relationship with pressure at a constant temperature.  $B_w$  changes linearly as it approaches  $P_b$  and if the pressure falls below  $P_b$ ,  $B_w$  continues to

increase at a slowing rate. In general, by decreasing the pressure, geothermal fluids will expand and thus increase in volume.



**Figure 10:** Formation Volume Factor of Water (McCain, 1990).

The following equation represents B<sub>w</sub>.

$$B_w = (1 + \Delta V_{wp})(1 + \Delta V_{wT})$$

$\Delta V_{wp}$ =change in volume due to pressure reduction  
 $\Delta V_{wT}$ =change in volume due to temperature reduction

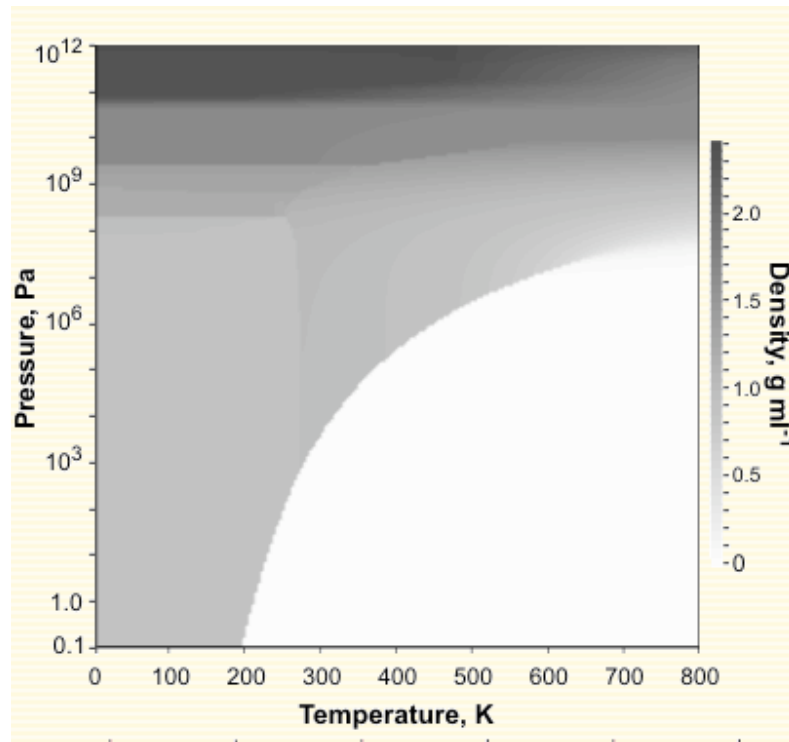
Determination of  $\Delta V_{wp}$  and  $\Delta V_{wT}$  rely on published correlations published in the Chemical Engineer's Handbook. The entire calculation process as outlined by McCain (1990). Also, the gas formation volume factor, B<sub>g</sub>, may be calculated in systems involving only the gas phase. The total formation volume factor, B<sub>t</sub>, may be calculated in two-phase systems such as a liquid – vapor reservoir.

#### 3.4.4.4 Density

The density of a geothermal fluid is a function of its TDS, temperature, and pressure. Fluid densities have impacts on production infrastructure such as electric submersible pump (ESP) sizing. Calculation of geothermal fluid density again relies upon tabulated correlations, which are based upon equations of state (EOS).

$$P_w = P_{w@STP}/B_w$$

See McCain (1990) for a detained explanation for calculation of density. **Figure 4** shows density of water as a function of temperature and pressure.



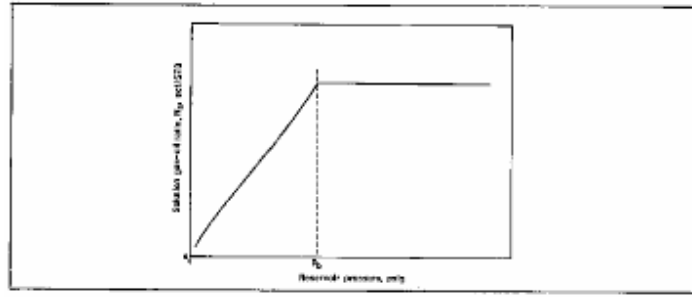
**Figure 11:** Density of water at different pressures and temperatures (Chaplin, 2009)

#### 3.4.4.5 Solubility of Gas in Geothermal Fluids

In many geothermal systems there exist volumes of dissolved gases in solution at depth. It is important to consider the effects of a changing pressure on the fluid being analyzed. The solution gas – water ratio,  $R_{sw}$ , is defined as the following:

$$R_{sw} = \frac{\text{Volume of gas produced at surface at standard temperature and pressure/}}{\text{Volume of liquid entering production infrastructure at standard conditions}}$$

The bubble point pressure of a system again affects this property. If the pressure is above the bubble point, then the liquid is fully saturated and will not dissolve any more gas into solution. If the pressure falls below the bubble point, then gas will evolve from the liquid into the pore space (or production line), which reduces the amount of gas dissolved in solution (McCain, 1990). **Figure 5** shows the importance of bubble point pressure related to solubility



**Figure 12:** Solubility Curve related to pressure (McCain, 1990)

#### 3.4.4.6 Coefficient of Isothermal Compressibility of Water

Isothermal compressibility of water,  $C_w$ , is defined as changes in fluid volume per change in fluid pressure. Calculation of  $C_w$  is highly dependant upon if a pressure is above or below the bubble point pressure. At the bubble point, there exist a discontinuity that is reflected in the following equation.

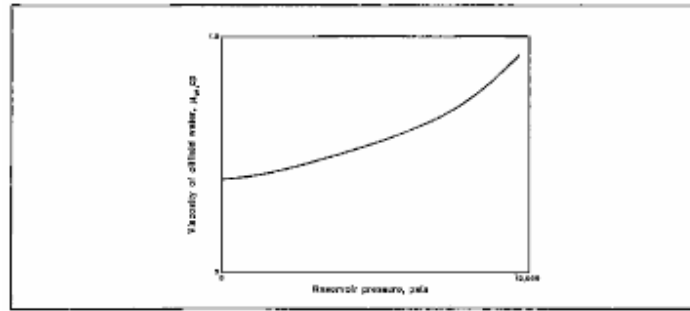
$$C_w = -1/V_{\text{water}} * (\Delta V_{\text{water}} / \Delta P)_{T=\text{constant}} = -1/B_w * (\Delta B_w / \Delta P)_{T=\text{constant}} \rightarrow \text{Above Bubble Point}$$

$$C_w = -1/B_w * (\Delta B_w / \Delta P)_{T=\text{constant}} + B_g/B_w * (\Delta R_{sw} / \Delta P)_{T=\text{constant}} \rightarrow \text{Below Bubble Point}$$

The derivatives involved in these equations are established using published correlations in most cases. TDS counts have an impact on  $C_w$  as well. Water compressibility must be corrected depending on percentages of dissolved solids. This calculation procedure is outlined by McCain (1990).

#### 3.4.4.7 Viscosity

The viscosity of water,  $\mu_w$ , is defined as the measure of resistance to flow (McCain, 1990). Viscosity is highly dependant upon reservoir temperature. Field data indicates that viscosity has little dependence upon pressure. Only minimal changes will occur due to pressure changes. Typical oilfield waters have absolute viscosities of less than 1cP (Centipoise). **Figure 6** illustrates the typical viscosity of water as a function of reservoir pressure.



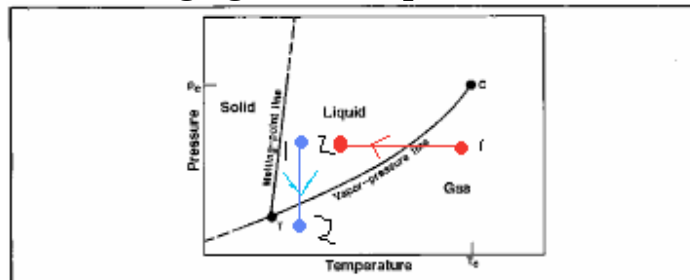
**Figure 13:** Viscosity of brine water (McCain, 1990)

Viscosity influences flow rates in and out of the reservoir. Viscosity can be calculated in the laboratory using a rolling ball viscometer.

### 3.4.4.8 Enthalpy

The enthalpy of a reservoir fluid is important regarding thermodynamic considerations. Enthalpy is a function of pressure and temperature in two-phase systems. The state of a reservoir can be fully determined using these properties. Enthalpy is also used in calculation of heat and work associated with the First Law of Thermodynamics (Eliasson and Kjaren, 1983). A rigorous discussion of fluid enthalpy is beyond the scope of this paper.

### 3.5 Implications of Changing Fluid Properties



**Figure 14:** Possible shifts in fluid state if reservoir temperature and pressure are changed

**Figure 7** above illustrates possible changes in fluid state if reservoir temperature or pressure is modified. For example, if a reservoir pressure is reduced a fluid dominated reservoir may become more vapor dominated. Other scenarios, such as temperature reduction, may lead to a shift from a gas-dominated state to a liquid dominated state. These types of effects can have implications on production rates and surface infrastructure (designed for one type of reservoir only).

### 3.6 Heat Flow in the Reservoir

Heat,  $Q$ , may be transferred within a reservoir in three different ways.

1. Dispersion
2. Conduction (Diffusion)
3. Convection

Heat dispersion in a reservoir relates to the mixing of fluid within reservoir pore space. This allows for heat transfer between molecules. Dispersion typically has little overall impact on heat flow. Conduction (or Diffusion) is described as heat transfer occurring over a stationary medium if locations within the medium vary in temperature (Harb and Solen, 2005). Heat conduction will occur between water molecules in the reservoir as well as between the stationary heat source (hot rock) and bordering liquid. For example, molecules closer to the source of heat will transfer heat to molecules on their margins and then to other nearby molecules. Heat conduction is governed by Fourier's Law of Heat Conduction:

$$Q_{\text{conduction},x} = -k \cdot A \cdot (\Delta T / \Delta x)$$

K = thermal conductivity of a material  
A = cross sectional area  
 $\Delta T$  = change in temperature across medium  
 $\Delta x$  = distance between points of interest

•	Granite 1.73–3.98 W/m-°C
•	Limestone 1.26–1.33 W/m-°C
•	Marble 2.07–2.94 W/m-°C
•	Sandstone 1.60–2.10 W/m-°C

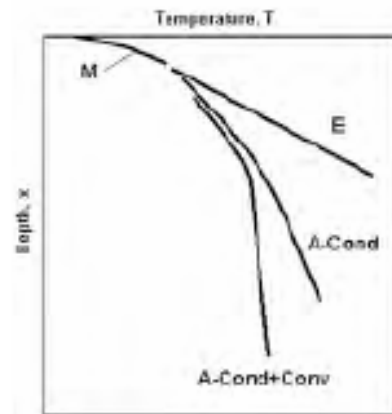
**Table 2:** Typical thermal conductivities of common lithologies. From Dipippo(2007).

Convection occurs when a fluid flows along a surface and the temperature of the surface and fluid are different (Harb and Solen, 2005). The following equation governs heat convection.

$$Q_{\text{convection}} = A \cdot h \cdot (T_r - T_l)$$

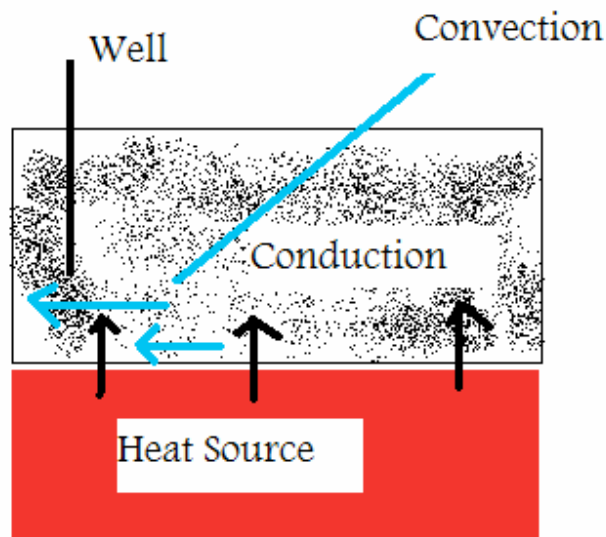
A = cross sectional area.  
h = heat transfer coefficient  
 $T_r$  = temperature of the rock  
 $T_l$  = temperature of the liquid

In many cases, due to relatively small temperature changes associated with low velocities of the fluid,  $T_r = T_l$  and thus this term is negligible. Forced convection occurs when a cooler liquid is injected into the reservoir. Natural convection can occur due to density difference between the fluid within a reservoir (Eliasson and Kjaren, 1983).



**Figure 8:** Depth relationship with heat transfer mechanism. From Dipippo (1997).

**Figure 8** above shows how heat flow in deeper formations relies on both convection and conduction, while heat flow in shallow formations may be only controlled by conduction.



**Figure 9:** Schematic of conduction and convection within a reservoir

**Figure 9** illustrates a general model of convection and conduction within a reservoir.

## 4.0 Reservoir Calculations

In order to determine the viability of any reservoir, several basic calculations must be made. These calculations are all related to the five aforementioned elements of a commercially viable geothermal resource.

### 4.1 Volume

The calculation of reservoir volume relies upon several of the previously developed variables. The following equation, modified from Graves (2008), governs volumetric reservoir calculations.

$$V = C * A * h * (S_w) * \phi * RF / B_w$$

$C$  = unit conversion  
 $A$  = Aerial Extent (acres)  
 $H$  = height of the formation  
 $S_w$  = Water Saturation (%)  
 $\phi$  = Porosity (%)  
 $RF$  = Recovery Factor  
 $B_w$  = Formation volume factor of water (res. Bbl/STB)

In the case of a geothermal reservoir, this volumetric equation may be used to evaluate the overall volumes of water that exist for a particular resource. It may be used as a starting point for decline calculations (if re-injection is not used) .

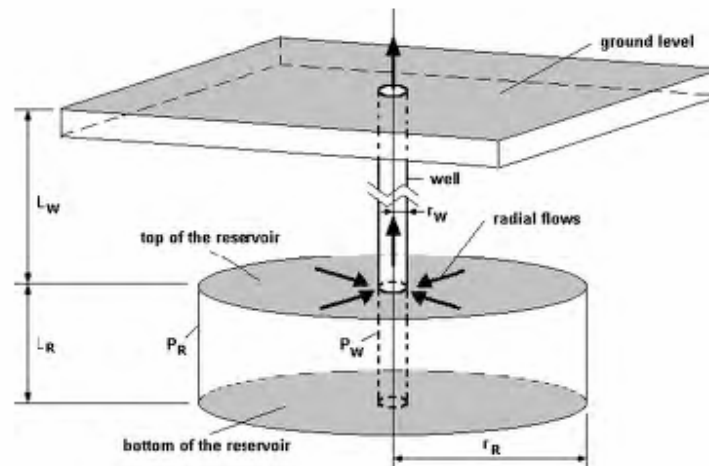
## 4.2 Flow Rate Calculations

Similarly, to the oil and gas industry, having an adequate volume of fluid is not enough to make it a commercial resource. A reservoir must have adequate in-flow and out-flow from the reservoir. Darcy's Law governs fluid flow through porous media. There are several important forms of Darcy's Law that are useful in different scenarios.

1.  $Q = (-k * A / \mu) * (\Delta P / L + \rho g * \sin(\alpha))$ , where  $\alpha$  = bedding dip angle
2.  $Q = (k * h * \Delta P / 141.2 * \mu * B_w) * (1 / (1/2 * \ln(10.06 * A / C_A * r_w^2) - 3/4 + S))$   
 $K$  = permeability (mD)  
 $Q$  = flow rate ( STB/day)  
 $A$  = reservoir drainage area (ft<sup>2</sup>)  
 $C_A$  = shape factor for specific drainage area (-)  
 $R_w$  = bore hole radius (ft)  
 $S$  = skin factor (-)  
 $\rho g$  = .433psi/ft \* Fluid specific gravity

Two forms of Darcy's Law have been presented about. The first equation relates dip angle in beds to calculation of flow rate. This intrinsically incorporates the notion of pressure head. The second equation, developed by Lee(1982), is a generalized equation for flow over a general area. Various drainage shape factors, developed by Dietz (1965), are tabulated in **Appendix A**.





**Figure 10:**General radial flow into wellbore (Dipippo, 2007)

It must be emphasized that Darcy's Law can be modified for a variety of physical situations. The form it takes will depend upon the flow regime (flow pattern into wellbore based on physical situations), which can be radial, linear, bilinear, steady state, pseudo-steady state, and several others. For example, linear flow is more common initially in highly fractured formations or following fracture stimulation (Chaudhry, 2003). Chaudhry (2003) argues that in time all wells reach so called pseudo-radial flow. Darcy's Law may also be modified to include two phase fluid effects (Kjaran and Eliasson ,1983). **Figure 10** shows a general flow regime into a reservoir wellbore.

In reality, flow rates are typically measured directly by using flow meters, pressure transient analysis, and a host of other techniques used by the oil and gas industry that are applied to geothermal systems. The obtained is then interpreted to determine flow regime and to predict future flow regimes. The table in Appendix A, which was adapted from Buchwalter et al (2008), illustrates various flow regimes and corresponding physical situations. In the context of a geothermal reservoir, the most likely flow regimes would be the dual porosity model, dual permeability, communicating faults, the intersecting faults model, and pseudo-radial flow.

## 5.0 Reservoir Types

There are several types of geothermal reservoirs. Each type has different properties and will have different reservoir calculation techniques. The details of the differences will not be presented in this paper as it is beyond the scope of this introduction. The three main types of geothermal reservoirs include (Dipippo, 2007; Eliasson and Kjaran, 1983):

1. Vapor Dominated Reservoir
2. Fluid Dominated Reservoir
3. Hot Dry Rock (HDR)
4. Geo-Pressured

In vapor-dominated reservoirs, the vapor phase is the most continuous and it governs the pressure regime of the reservoir. Liquid that is present in the reservoir may be immobile and thus unable to flow. Due to the fact that there exists less fluid in this type of

reservoir, the overall heat transfer will be lower than a liquid dominated reservoir since vapor does not conduct heat well. However, production infrastructure will last much longer due to less corrosion caused by high TDS or bacteria downhole. The most famous examples of this type of reservoir are in Ladarello, Italy and The Geysers, CA (Dipippo, 2007)

Liquid dominated reservoirs have a liquid phase, which is the most continuous phase. These reservoirs will require complex calculations to account for vapor and liquid effects in heat flow and production. These type of reservoirs must be closely monitored for changes in production patterns due to changes in the reservoir properties caused by production. This type of system typically produces moderately hot geo-fluid (Dipippo, 2007).

Aamodt (1973) developed the Hot Dry Rock (HDR) model during the 1970s. This model suggests that if a fluid is pumped downhole deep into a hot formation, then heat transfer will occur and the heated fluid can be produced. This is known as an artificial reservoir. This type of model was the basis for EGS models of today (Dipippo, 2007).

Geo-pressured reservoirs exhibit very high reservoir pressures. These pressures can exceed hydrostatic pressure (.433 psi/ft) and in some cases can reach as high as 1 psi/ft. During research, there was little data available to determine the success or failure of this type of reservoir (Dipippo, 2007).

## **6.0 Fracture of Rock**

In the oil and gas industry many reservoirs contain sufficient volumes of hydrocarbons, but lack permeability. This problem is handed through fracturing the formation. The goal of any “frac-job” is to increase permeability to the wellbore and decrease skin effect, which may have been caused during the drilling process. This will effectively “stimulate” the reservoir. The same type of logic can be applied to geothermal reservoir stimulation.

The mechanics of rock are particularly important for both understanding the reservoir and for stimulation purposes. Unlike any man-made or fabricated material, rock is not made to any particular prescribed specification. Reservoir rock has a history involving appreciable mechanical, thermal and chemical actions over millions of years. In order to better understand the reservoir, reservoir rocks and surrounding formations must be extensively studied and analyzed from field and laboratory tests.

The common characteristics of rock materials can be summarized with reference to the following four aspects (Aliabadi, 1999: Whittaker et al, 1992: Wyllie and Mah, 2001).

1. Discontinuity: which commonly refers to the joints, cracks, pore spaces and other natural weaknesses within the rock.
2. Heterogeneity: which refers to a measure of the physical non-uniformity of a material and has by implication a sense of scale
3. Anisotropy: which refers to a measure of the directional properties of a material.

4. Permeability: which refers to the property of a rock to allow its transmission of water or other fluid through its structure

These principles govern how reservoir stimulation techniques are designed and implemented. A more rigorous discussion of fracture of porous materials is discussed in **Appendix A**.

## **7.0 Reservoir Recharge and Injection Processes**

In any geothermal reservoir, a recharge for the fluid is needed for the resource to be sustainable over time. In many cases recharge mechanisms are related to high topographic relief above the margins of a reservoir. Water from precipitation recharges through fractured rock and permeable layers of stratigraphy. During production, if there is not proper reservoir management, the reservoir pressure may be reduced and this can cause many implications involving the fluid properties. Over time, the reservoir may become less productive or even unproductive. This is the reason behind the idea of re-injection of geo-fluids.

Injection well design considers a variety of factors to properly recharge a reservoir and thus keep reservoir pressure stable. Injection well placement is critical to allow proper “sweep” within the reservoir. Injection well placement is determined mainly by investigation of seismic data and geological structure. Reservoir heterogeneity must also be investigated to ensure that injected fluid actually reaches the volume within the reservoir that must be re-pressured (Craig, 1971).

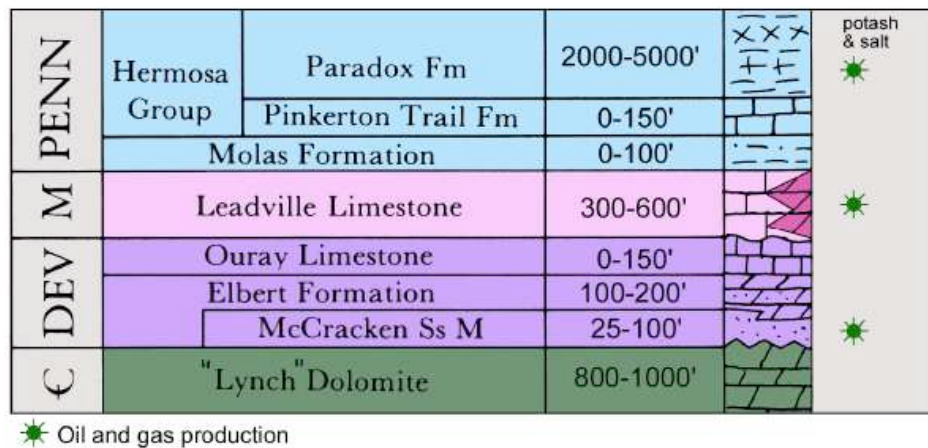
## **8.0 Case History**

Just as in any aspect of geothermal engineering proper case studies are crucial to interpretation of the system being analyzed. From a reservoir engineering point of view, similar regional geology and similar fluid properties must be considered in order to develop a model that goes beyond hypothesis. Analogous situations should be determined in order to reduce risk involved during exploration and infrastructure development.

## **9.0 Rico Reservoir Model**

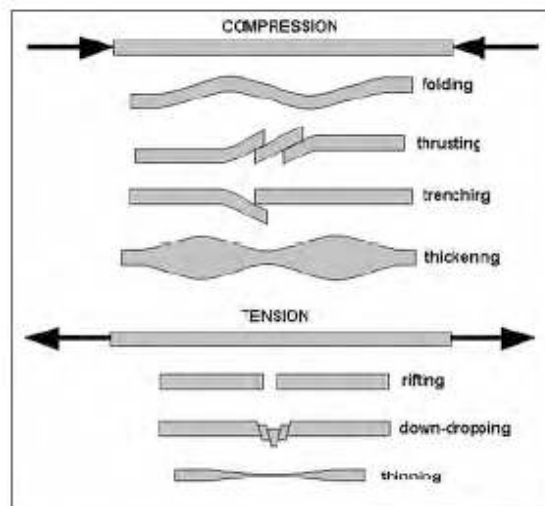
### **9.1 Geological Setting**

The geology in Rico area and surrounding areas is highly complex. During the Pennsylvanian period, the Paradox basin extended from eastern Utah into the San Juan Basin. It is evident that this type of basin existed due to the outcrops of Pennsylvanian formations such as the Hermosa and Leadville formations (Mississippian formation) in Ouray and in the vicinity of Rico (Brown, 2002). The MegaMoly Report (2009) suggests that the source of geo-fluid may be from the Leadville Limestone and the Hermosa formation. The regional stratigraphic sequence is presented in **Figure 11** and in **Appendix B**. These two formations outcrop in some areas near Rico indicating that beds dip at extreme angles.



**Figure 11:** Stratigraphy of possible Rico reservoir formation (UGS, 2007)

Two major igneous intrusions have greatly modified the stratigraphy of the region. The first event occurred during cretaceous age and the second event occurred during the Pliocene. Rico is situated near the center of the Rico Dome, a prominent east-west trending faulted anticline that has Precambrian greenstone and quartzite at its core and Paleozoic clastics and carbonates on its northern and southern flanks (Knight, E.T., 1974). The elliptical dome, formed during the Pliocene, is approximately 8 kilometers long, and corresponds well to the eastern lobe of a prominent magnetic high (Anaconda, 1980). This Pliocene volcanism caused massive igneous intrusions with associated rhyolitic dikes and faults. This upward lifting has caused massive east-west trending faults with an overall anticlinal structure. This pattern has produced a graben-like, thinning and down dipping, fault block pattern as the crust was faulted and pulled apart by the intrusion. The following figure, **Figure 12**, illustrates this pattern.



**Figure 12:** Typical effects of tectonic events on crust (Dipippo, 2007)

The cross-section taken across the Rico valley, shown in **Appendix B**, shows a similar, but much more complex pattern of graben-structures that have been turned by further faulting in the area. It is possible that these faults provide a conduit between the underlying reservoir (s) and the surface. There is a lot of surface evidence of geothermal activity, which is evident by the numerous hot springs across the Rico quadrangle.

## 9.2 Possible Formation Top Determination

Based upon previously collected data by the USGS (1983), the Rico Dome has created approximately 3,000 feet of upward relief. Well logs immediately west of Rico show Leadville Limestone formation tops of 6,400 feet to 7,700 feet (from top of well). On both the northeast and southeast regions of the geologic map of Rico (**shown in Appendix B**), the Leadville Limestone and Hermosa Formation outcrops. This indicates that the formation “top” may lie on a steep dip angle and the reservoir itself may be tilted due to the heavy faulting across the region.

## 9.3 Well Log Data

Geophysical data and interpretation from and the Colorado Geological Survey (2009) and Medlin(1983) indicate that the geology in the Rico area supports a geothermal resource.

Data indicates large variations in gravity, which could indicate extensive faulting and flow conduits. The data also indicates regions of high heat flow in and around the town of Rico. Heat flow values range from 217 to 288 mW/m<sup>2</sup>, which shows that the Rico geothermal resource will provide an adequate heat source (MegaMoly, 2009). Heat flow and gravity maps are shown in **Appendix B**.

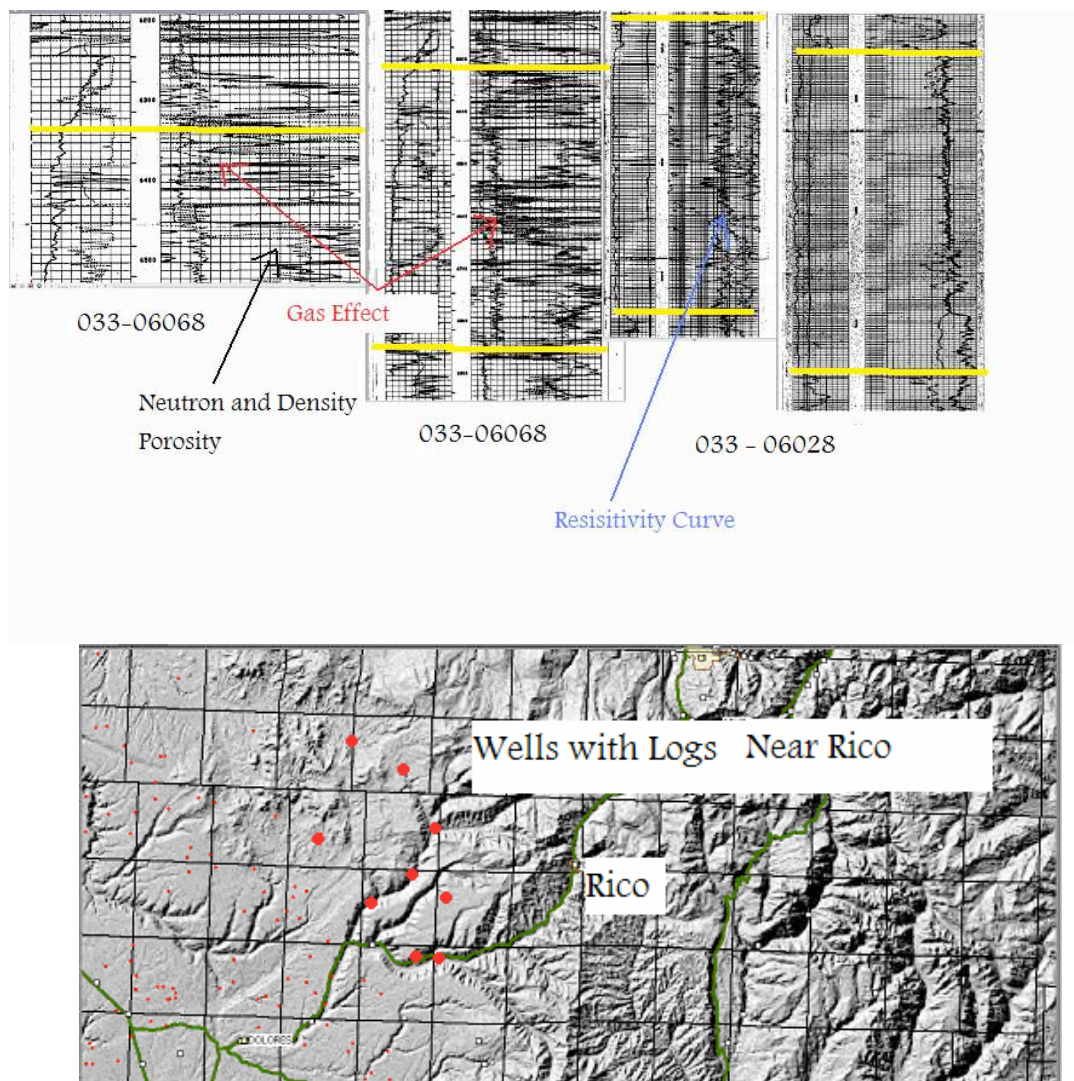
Unfortunately, there have been few wells drilled near the Rico geothermal reservoir aside from three shallow exploratory wells drilled by mining companies over the years. Medlin (1983) presents some down hole temperature data. Temperatures ranged from about 66°C to 77°C. These drill holes were drilled to between 1500 m – 1600 m in depth. Well Logs, if run, were not provided and were not available for interpretation.

While there is no well log data available directly in Rico, there exist hundreds of thousands of gas wells over the San Juan Basin. Several nearby well logs were obtained from the Colorado Oil and Gas Conservation Commission database. **Figure 13** shows several log sections of wells within 15 miles of Rico. **Appendix B** contains a typical log section of the Leadville Limestone from the Lisbon Field, Utah.

Due to such a lack of data across the region, formation tops of the Leadville Limestone were simply picked by log response correlation from other wells eastern Utah in the Paradox Basin. Gamma ray showed the most distinctive response considering such a low API value and the extreme thickness of Leadville Limestone in areas west of Rico. The isopach map shown in **Appendix B** illustrates thickness of 100 feet to 300 feet thick over the central portions of Delores County. Based off of other Well logs and data Chidsey et al (2007) showed that the Leadville Limestone thickness ranges from 200 ft to 700 ft

across the Paradox Basin, with average intergranular porosities of 6% - 8% from core data.

The values obtained from the well logs shown in **Figure 13** ranged from <5% to over 30%. These values were read directly off neutron porosity or neutron density well logs. It is likely that these porosity values are closer to the actual porosity since core derived porosity does not include fracture porosity. It is also possible that since the cores are not from the same logged wells, that there has been heavy chemical diagenesis resulting in lower porosity. In addition, several of the log sections show the “gas effect” (cross-over of neutron density/density porosity log), which indicates the presence of gas in the pore space. This result agrees with geochemical observations that the fluid appears to contain high concentrations of CO<sub>2</sub>.








**Figure 13:** Log sections and well locations near Rico (cogcc, 2009)

Permeabilities derived from core data in the Paradox basin show a range of values between 20 mD to a few hundred mD (UGS, 2007;USDI, 2006). Permeability across the Leadville Limestone is highly variable due to local chemical diagenesis and possible vugs that exist in limestone lithologies.

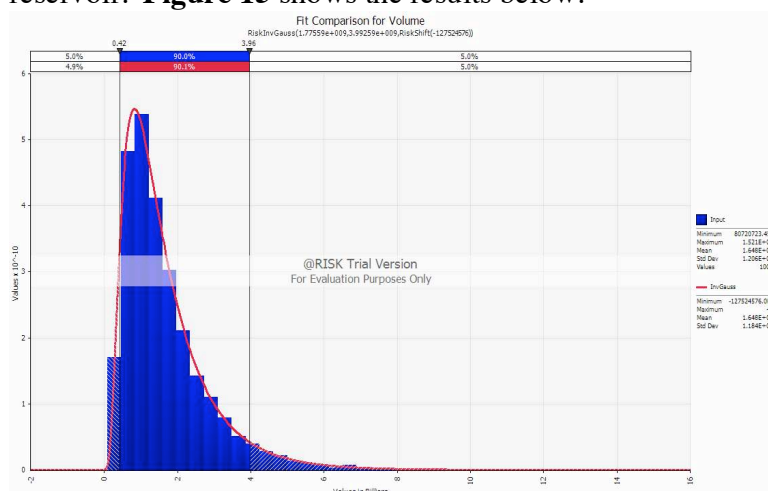
## 9.4 Volumetric Calculations

Using the volumetric equation specified above and Palisade Software's @Risk 5.0, a Monte Carlo Simulation was performed. A lognormal distribution was used for both porosity inputs, which is common in geostatistical analysis. The aerial extent, A, used a triangular\_distribution. Water saturation,  $S_w$ , was assumed to have a normal distribution. These parameters were used since we are dealing with a fluid dominated reservoir and most geothermal reservoirs are fully saturated with little variance. **Figure 14** shows all of the inputs and distributions for the variables needed for the volumetric calculation.

Simulation Results For Outputs:									Inputs= 4, Outputs= 5
Name	Cell	Graph	Min	Mean	Max	5%	95%	Errors	
[- Range: phi									
phi	B5		4.212846E-02	0.1499996	0.5085732	8.342168E-02	0.2426614	0	
h	B6		16.14008	150.0011	924.6495	61.66975	291.7451	0	
A	B7		515.9606	1866.667	3498.468	905.8605	2965.743	0	
Sw	B9		0.9861516	0.9900001	0.9943588	0.9883548	0.9916441	0	
[- Range: <none>									
Volume	B3		8.072072E+07	1.64807E+09	1.521494E+10	4.197401E+08	3.95628E+09	0	

**Figure 14:** Inputs for Volumetric Monte Carlo Simulation

The average reservoir volume attained after 10,000 simulations was about 1,650,000,000 ft<sup>3</sup> of in place water. The output distribution was lognormal. Data was not obtained in order to determine if this is a reasonable estimate for water volume in a geothermal reservoir. **Figure 15** shows the results below.



**Figure 15:** Volumetric output using a Monte Carlo Simulation



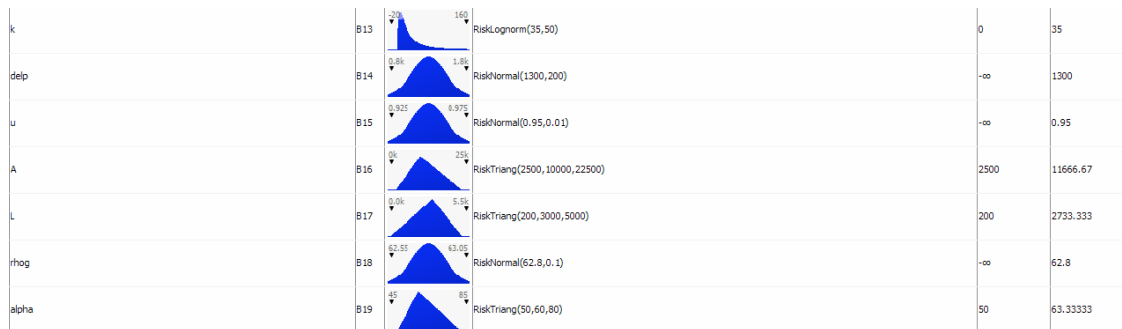
## 9.5 Flow Rates and Associated Calculations

There appear to be some flow rate data from surface geothermal features in the area. It is encouraging that there is natural flow to the surface out of the reservoir. Natural flow indicates good permeability from the reservoir to the surface. Newer flow rate measurements should be taken to confirm that the reservoir has not lost pressure and thus incurred a decreased production flow rate. **Table 3**, which summarizes data obtained by Pearl (1979), shows some of the natural flow rates from springs across the Rico area.

Location	Flow Rate, Q, gpm
Dunton Hot Springs	25
Paradise Warm Springs	28 - 34
Geyser Warm Springs	20 -250
Rico Hot Springs	15
Big Geyser Warm Springs	8-12
Little Geyser Spring	15

**Table 3:** Flow rates from springs near Rico (Pearl, 1979).

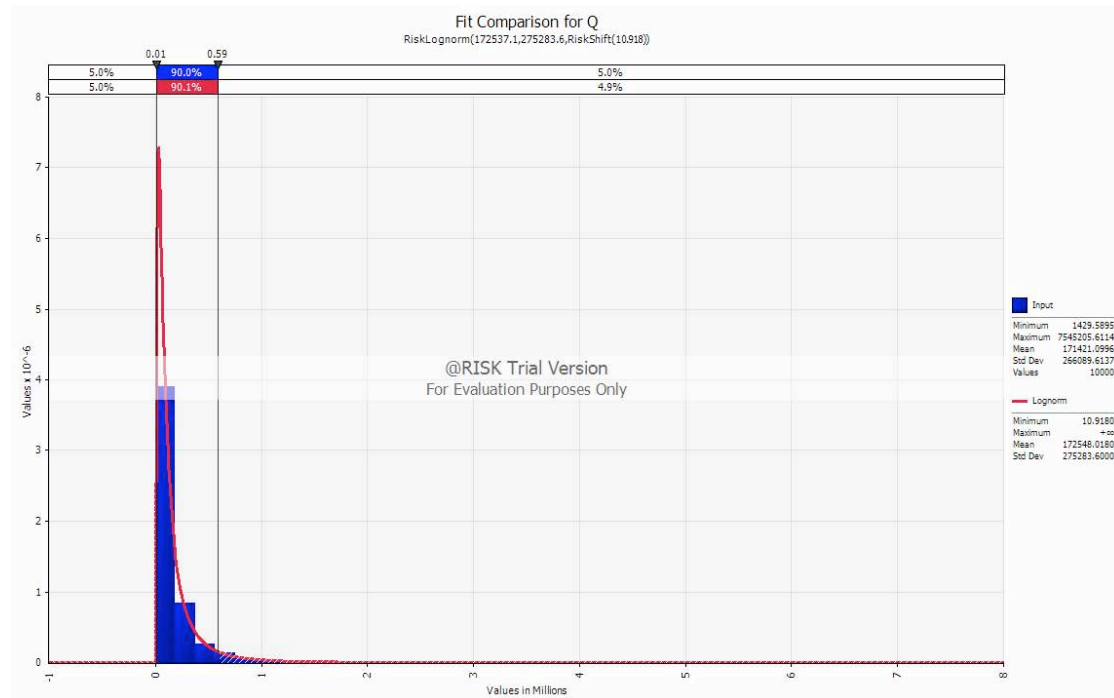
A Monte Carlo type simulation was conducted using @Risk 5.0 for possible flow rate determination. Permeability was governed by a lognormal distribution, which is standard in other geostatistical models. The other variables used normal and triangular distributions. **Figure 16** summarizes the input variables.



**Figure 16:**Inputs for flow rate calculation using Monte Carlo Simulation

The average (50<sup>th</sup> percentile) flow rate was about 170,000 bbl/day, which is roughly 8.15 cfs. This appears to be a relatively good indication of possible flow rates to expect. If the reservoir were pumped, flow rates would be expected to dramatically increase and could potentially support an large increase in usage for either direct usage or power plant applications. **Figure 17** shows the output using @Risk 5.0 below.





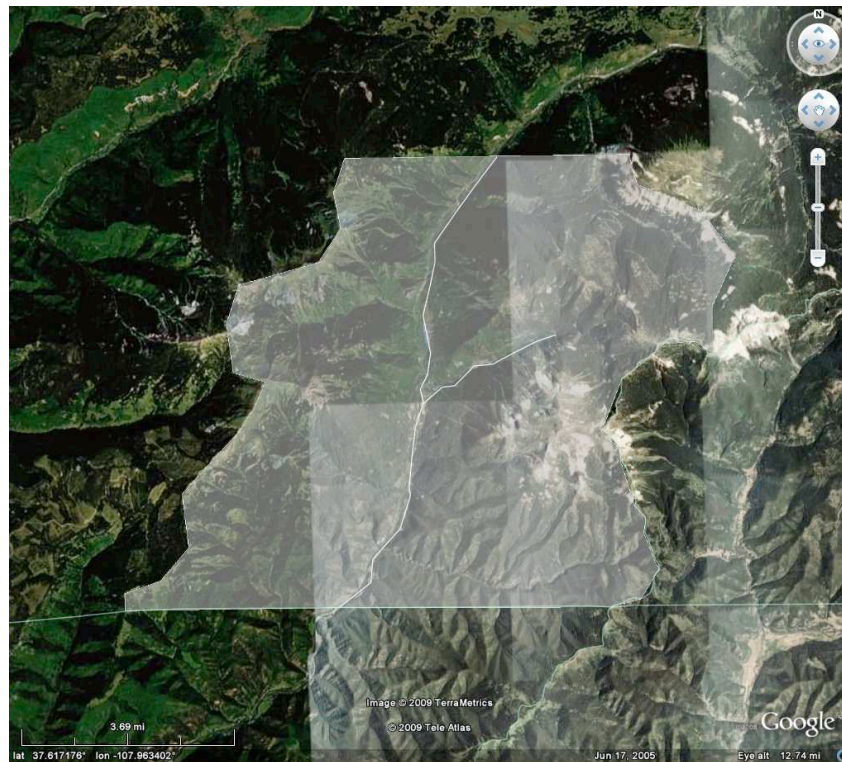
**Figure 17:** Flow rate output using a Monte Carlo Simulation.

## 9.6 Recharge Model

A conceptual fluid re-charge model was built using Tecplot Focus, an engineering plotting software product. In order to build the model, many assumptions had to be made. These assumptions were necessarily broad due to the lack of data for the region. A general geologic layout was determined based off of the following studies. Contacts between the greenstone and Uncompahgre Quartzite, and between the Uncompahgre and the Hermosa Formation, appear to have been conduits for mineralizing fluids (Cameron, et al., 1985). A younger Pliocene event (3.4 to 4.5 Ma) that emplaced basaltic, andesitic, rhyolitic and lamprophyric dikes was associated with a hydrothermal system and base and precious metals mineralization. The hydrothermal mineral deposits include Ag-Zn-Au epithermal veins, limestone replacement Cu-Ag-Au deposits (e.g. “NBH” deposit in the Leadville Limestone) just north of town, and a porphyry Mo deposit about a 1.6 km east of town (Cameron, et al., 1985). The Pliocene intrusive event formed a hydrothermal plume (termed the Rico Paleothermal Anomaly or PTA) above the porphyry Mo deposit that was 3 km wide and at least 2 km high, and produced alternation patterns that extended out up to 8 km (Larson, et al., 1994). The data indicate that significantly elevated geothermal gradients ( $>90$  °C/km) are not restricted to a single area, but have widespread occurrences, with an area encompassing the anomalous gradients extending a minimum of 2.5 km north to south and 1.6 km west to east (Ausburn Geoscience, 2009). Based on these studies, the area of interest was identified to be within the Rico basin, so a

topographic surface water catchment basin was created to calculate the total water influx into the system.

This basin was estimated by the mountain ridges surrounding Rico, although it is possible that the total recharge area is larger. Based on a mean annual precipitation of 23.69 in/year at the Telluride Airport (KTEX) and a total catchment basin area of 1,588,672,207 square feet, the total water influx in the basin was determined to be 27.65 cfs over all points within the region. The average, of the 50 year average by day, flow of the Dolores River was 132.79 cfs measured just below Rico(USGS, 2009). Without knowledge of the flow rate of the Dolores River into the Rico valley and without full understanding of the water table, fluid dynamics, and catchment basin, it is not possible to perform the complete mass balance for the system. **Figure 18** outlines the approximate catchment basin.



**Figure 18:** Hypothesized catchment Basin (Tecplot and Google Maps)

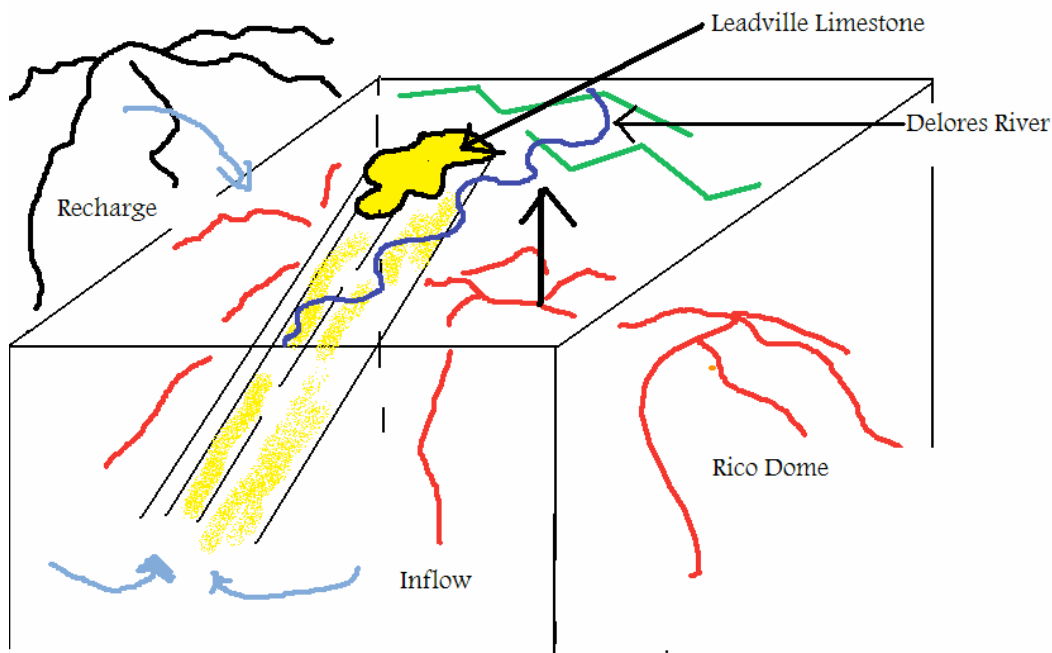
## 9.7 Re-injection Possibilities

In order to maintain a stable geothermal system, the possibility of injection wells must be considered. Care must be made to placement in areas where wells will intersect extreme dip angled beds. An updated understanding of subsurface faulting and structure should be obtained before injection well placement can be determined. If possible, a seismic survey should be shot over the Rico geothermal region.

## 9.8 Case Study

Unfortunately, after extensive research there has not been a valid case study that relates well to the geology and possible reservoir in Rico. There are loose connections between the fluid properties (low temperature fluid and low TDS) between Rico and the geothermal system in Boise, Idaho. However, geothermal fluid in each situation evolves from entirely different formations as well as having somewhat varied geology and geography. There appear to be some similarities between large amounts of small scale faulting. It will be important in the future to determine a case study as a starting point for characterizing the Rico reservoir.

## 9.9 Reservoir Characterization



**Figure 19:** Schematic of possible Rico geothermal reservoir

**Figure 19** shows the possible Rico reservoir based off of limited data. The reservoir fluid flow is likely driven by  $\text{CO}_2$  gas that has evolved from chemical alteration of the Leadville Limestone. Both geochemical and surface data indicate a strong presence of  $\text{CO}_2$  in the geo-fluid. Due to the surface data and known cross sections, the beds are likely steeply dipping and may or may not be discontinuous at depth. Recharge evolves mainly from the surrounding San Juan mountains and potentially from the Delores River. Much is still misunderstood regarding the reservoir in Rico. Data must be collected and analyzed in order to either reject or expand on the current model.

## 10. Future

In order to successfully develop an accurate conceptual reservoir model the following should be obtained:

- Reservoir rock properties and reservoir fluid properties
- Drill a Slim hole (relatively inexpensive test well to gather this data-core samples, downhole fluid properties)
- Determine underground fault structure and formation continuity using seismic if possible
- Perform hydrologic study on possible catchment basin and possible recharge mechanism
- Find a relevant case study to better understand possible reservoir models for Rico

## 11.0 References

- Aliabadi, Fracture of Rock, 1999.
- Aamodt. Artificial Geothermal Reservoirs in Hot Volcanic Rock. Geothermal Energy Group and Los Alamos Scientific Laboratory. 1973.
- Anaconda Copper Company, 1980. Aeromagnetic Map, Rico Project, Dolores County, Colorado.
- Asquith and Krygowski. Basic Well Log Analysis. AAPG Methods in Exploration, No. 16. 2004
- Brown. Outcrop to Subsurface Stratigraphy of the Pennsylvanian Hermosa Group, Southern Paradox Basin, U.S.A. Dissertation Louisiana State University. 2002.
- Brown, Brown, Freling, Nevermann. Rico Geology Report. CSM Geothermal Energy. 2009.
- Buchwalter, Iqbal, and Satter. Practical Enhanced Reservoir Engineering: Assisted with Simulation Software. PennWell Books. 2008.
- Cameron, D.E., et al., 1985. Discovery of the Silver Creek Molybdenum Deposit, Rico, Colorado. Society of Mining Engineers of AIME Transactions, Vol. 280, pp. 2099-2105.
- Chaplin. Water Phase Diagram. Accessed: 2 May 2009. from <http://www.lsbu.ac.uk/water/phase.html#den>.
- Chaudhry. Oil Well Testing Handbook. Elsevier. 2003.

Chidsey, Eby, Morgan, and McClure. The Mississippian Leadville Exploration Play, Utah and Colorado. UGS and Eby Petrography and Consulting, Inc. 2007.

COGCC. Well Log Images and Data. Accessed: April 2009. [oil-gas.state.co.us/](http://oil-gas.state.co.us/)

Craig. The Reservoir Engineering Aspects of Waterflooding. SPE. 1973.

Craft and Hawkins. Applied Petroleum Engineering. Prentice Hall. 1991.

Dietz. Determination of Average Reservoir Pressure From Build-Up Surveys. Journal of Petroleum Technology. Pg. 955-959. 1965.

DiPippo. Geothermal Power Plants: Principles, Applications, Case Studies and Environmental Impact 2<sup>nd</sup> Edition. Butterworth-Heinemann; 2007

GeoSociety. Rhyolite Data. Accessed 1 May 2009.  
[ftp://rock.geosociety.org/pub/reposit/2008/2008097.pdf](http://rock.geosociety.org/pub/reposit/2008/2008097.pdf)

Harb and Solen. Introduction to Chemical Processes 4<sup>th</sup> Edition. McGraw-Hill. 2005.

Knight, E.T., 1974. Geology and Ore Deposits of the Rico District, Colorado. United States Geological Survey Professional Paper 723.

Larson, P.B., 1987. Stable Isotope and Fluid Inclusion Investigations of Epithermal Vein and Porphyry Molybdenum Mineralization in the Rico Mining District, Colorado. Economic Geology, Vol. 82, pp. 2141-2157.

Lee. Well Testing 1<sup>st</sup> Edition. SPE Textbook Series Vol. 1. Society of Petroleum Engineering. New York and Dallas. 1982.

Mah and Wyllie. Rock Slope Engineering civil and mining, 2001;

MegaMoly Report. Business Plan for Geothermal Power Production Near Rico, CO. Prepared by Auburn Geoscience 2009.

Pearl, Richard Howard, 1979, Colorado's Hydrothermal Resource Base – An Assessment: Colorado Geologic Survey, Resource Series 6, Colorado Department of Natural Resources.

Santiseven. Southern Ute Indian Reservation. Red Willow Production. Accessed 2009.

United States Geological Survey (USGS), 2009. National Water Information System: Web Interface. [http://nwis.waterdata.usgs.gov/usa/nwis/dvstat/?site\\_no=09165000&por\\_09165000\\_6=345736,00060,6](http://nwis.waterdata.usgs.gov/usa/nwis/dvstat/?site_no=09165000&por_09165000_6=345736,00060,6)

United States Department of the Interior and US Forest Service. Oil and Gas Development and Reasonable Foreseeable Development (RFD) Scenarios in the San Juan National Forest and BLM Lands, Colorado. Prepared by Gault Group. 2006.

Utah Geological Survey (UGS). Deliverable 1.1: Core Descriptions, core photographs, and core analysis: Lisbon field, San Juan County, Utah The Mississippian Leadville Limestone Exploration Play, Utah and Colorado – Exploration Techniques and Studies for Independents. NETL (DOE). 2007.

Utah Geological Survey. Mississippian Madison Limestone, Uinta Mountains – Outcrop analog for the Mississippian Leadville Limestone Reservoir, Paradox Basin. 2008.


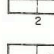

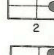

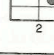


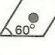
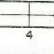
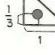
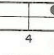
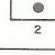

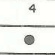


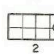

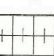

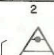


Whittaker et al. Rock Fracture Mechanics principles design and applications. 1992.

Acknowledgements: Dr. Kadri Dagedelen – Geostatistical Input and Dr. Mark Miller – Simulation Methods

Any Questions should be direction to team leader Jeff Reindl. He can be reached at [jreindl@mines.edu](mailto:jreindl@mines.edu)

## 12.0 Appendix A

Various Flow Regimes (Chaudhry, 2003)	
Flow Model	Comment
Wellbore Storage Effects	Early Time Signature
Linear Flow	Common in Stimulated Wells
Bilinear Flow	Common in Stimulated Wells
Dual Porosity	Common in Naturally Fractured Wells
Spherical Flow	Common in Partially Completed Wells
Pseudo-radial Flow	Most common effect
Constant Pressure Boundary	Constant support from gas cap or aquifer
Intersecting Faults	slope of line triples in semi-log plot between middle/late flow
Partially Communicating Faults	slope increases by factor of <2 on semi-log, corresponds to "hump" on dP plot
Dual Permeability	vertical cross flow in uncompleted layers

n bounded reservoirs	Stabilized conditions			n bounded reservoirs	Stabilized conditions		
	$\ln C_A$	$C_A$	for $\frac{kt}{\phi \mu cA} >$		$\ln C_A$	$C_A$	for $\frac{kt}{\phi \mu cA} >$
	3.45	31.6	0.1		2.38	10.8	0.3
	3.43	30.9	0.1		1.58	4.86	1.0
	3.45	31.6	0.1		0.73	2.07	0.8
	3.32	27.6	0.2		1.00	2.72	0.8
	3.30	27.1	0.2		-1.46	0.232	2.5
	3.09	21.9	0.4		-2.16	0.115	3.0
	3.12	22.6	0.2		1.22	3.39	0.6
	1.88	5.38	0.7		1.14	3.13	0.3
	0.86	2.36	0.7		-0.50	0.607	1.0
	2.56	12.9	0.6		-2.20	0.111	1.2
	1.52	4.57	0.5		-2.32	0.098	0.9
					2.95	19.1	0.1
					3.22	25	0.1

**Dietz Shape Factors (Lee, 1981)**

## Hydraulic fracturing of porous materials

Fracture of rock, including hydraulic fracturing technique, represents to the complete physical separation of two faces of a fracture due to excessive fluid pressure. This technique was originally developed to stimulate oil and gas reservoirs.

The classification and prediction of breaking processes within solid materials forms an extremely difficult problem in engineering science as well as in solid-state physics. This is true even for brittle materials exhibiting the simplest rheological behavior, i.e. no remnant deformations. Continuum mechanical treatments of brittle solids, based on Griffith's theory, are widely accepted in the scientific community and have shown good results in practical engineering applications. There are, however, a couple of problems associated with classical fracture mechanics, which limit its range of application. Certain restrictions arise from the assumption that the deformations can be conducted in a thermodynamically reversible manner. Connected to this is the basic assumption that the involved fracture processes are thermodynamic reversible too. This is usually expressed minimizing thermodynamic potentials with respect to crack or fracture growth, which is a perturbational scheme. The typical modeling situation is such that some governing field

equations are describing the global state of the deformation (i.e. the free energy density) according to some boundary or loading conditions while the free surface energy field (intrinsic strength) is classically assumed to be a constant property throughout the solid material. The assumption of a constant intrinsic strength constitutes a quite strong idealization for most experimental situations because it eliminates the field nature of cohesive properties. The assumption of a constant theoretical strength is most easily justified for homogeneous materials, i.e. perfect single crystals. However, even for such classes of materials there exist certain limitations: a) the crystal's cohesion is in general non-isotropic (variation in crystal strength according to crystallographic directions), and b) the cohesion is subject to thermal influences (lattice vibrations) introducing thermal fluctuations into the problem.

There are at least two different ways of implementing porosity numerically. In both cases certain micro structural elements (beams, plates or shells) will form a stress carrying elastic backbone. One can think, however, of two different realizations for the micro structural elements. The elements could be 'made' of a material which already follows the constitutive laws for porous materials, e.g. Biot's theory. This would be most satisfying from a continuum mechanical point of view as long as no fracturing occurs. However, if fracturing at the pore level is to be taken into account the above mentioned approach does not suffice (or even becomes inconsistent) and a micro mechanical approach must be employed. The pore space or volume has to be modeled explicitly in that case. We have focused on the latter implementation: the micro structural elements follow the classical constitutive equations of linear elasticity, and the pore space is viewed as the remaining vacant volume. The breaking of micro structural elements is associated with a coalescence of the pore volume under question. Because the pore volume is modeled explicitly the couplings between elastic and flow interactions ought to be derived explicitly from the micro structural configuration.

In the flow equations, a typical length  $l$  and thickness  $d$  and the liquid saturated equilibrium pore volume is simply  $(l-d)d^2$ . This states explicitly the considered material to be a binary system, i.e. any volume element is either occupied by elastic material or by pore fluid. By varying the ratio of  $l/d$  different values for the volumetric porosity can be achieved (ranging from nearly zero to nearly one). In order to obtain most simplified flow equations, we make the following assumptions: a) the pore fluid is incompressible (which appears well justified for water) and b) the fluid velocity relative to the bulk is proportional to the gradient of the pressure field (Darcy's relation). The continuity equations for solid and liquid mass density lead to the required pressure equation (in the continuum limit).

$$\text{div} (k/\mu * \text{grad } p) = \delta/\delta t \text{ div } u,$$

P = pressure  
u = displacement vector,  
k = mechanical permeability  
 $\mu$  = fluid viscosity.

This equation is a Poisson equation for the pressure field for constant  $k$  and  $\mu$ . The right hand side of the equation represents in general a time-dependent source term for the pressure field. It characterizes the local rate of relative volume change due to elastic deformations, and hence the net fluid fluxes itself. In general these net fluid fluxes will



control the pressure field's time-evolution. However, in this work we will only consider the stationary case. The physical motivation for this is the observation, that the characteristic internal relaxation time  $\tau = \mu/E$  for water-rock systems is typically of order  $10^{-6}$ s. It appears justified to assume that the time periods between successive breaking events are much larger than the internal relaxation time  $\tau$ , and hence that breaking events are triggered by stationary pressure and displacement distributions. In connection with the required pressure equation this implies balance of the net fluid fluxes for a given cell I to zero (Laplacian).

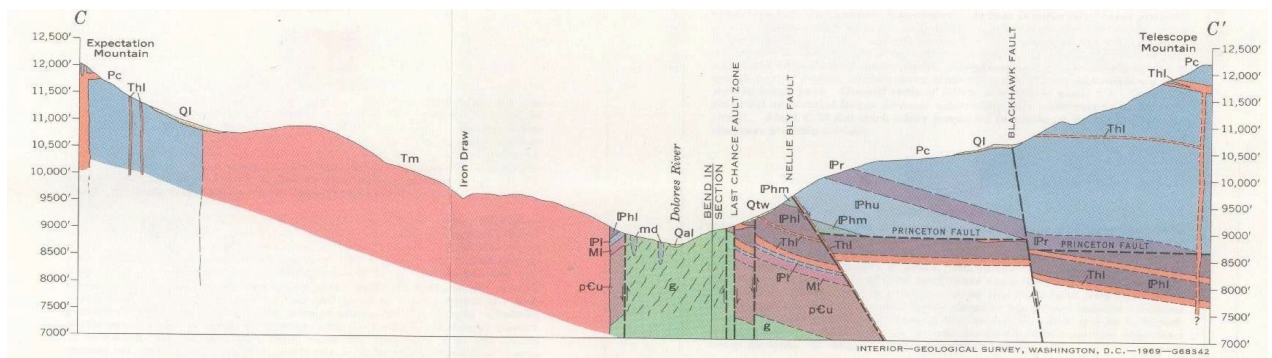
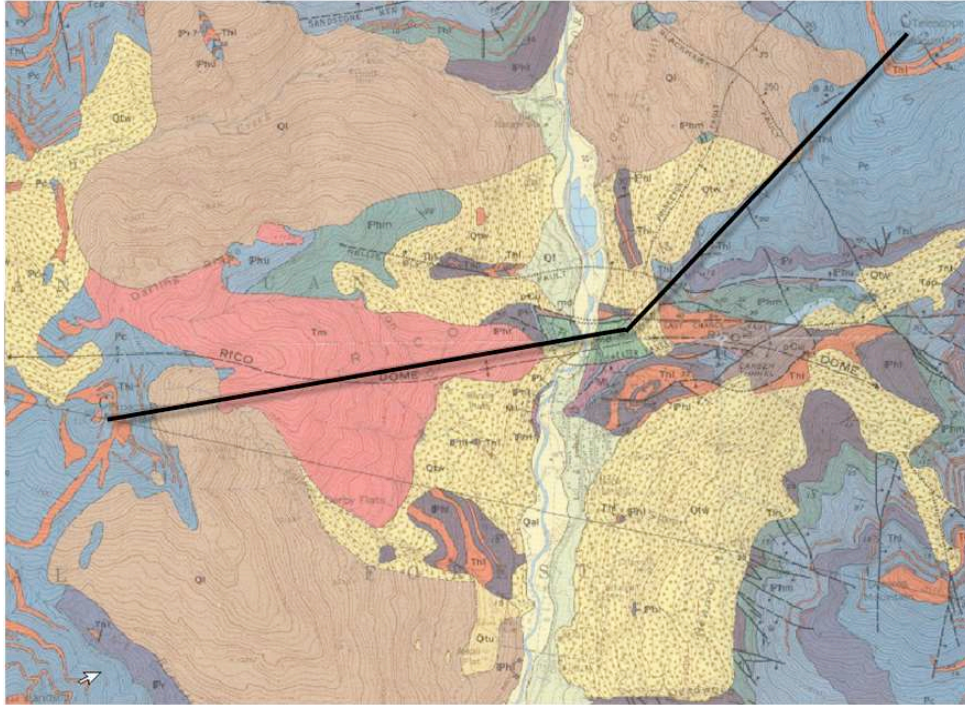
$$1/\mu \sum_j k_{ij}(p_i - p_j) + \text{boundary conditions} = 0$$

$k_{ij}$  = the local permeability across the beams (pore walls).

The pressure equation is solved without referring to any mechanical properties, which is a direct consequence of explicitly dropping all dynamic terms. Its solution for given boundary conditions represents the body force under which the elastic equations, among their own boundary conditions, are solved. Formally the corresponding continuum problem is analogous to the standard resulting stresses or strains and breaking thresholds we then determine which element(s) are broken next.

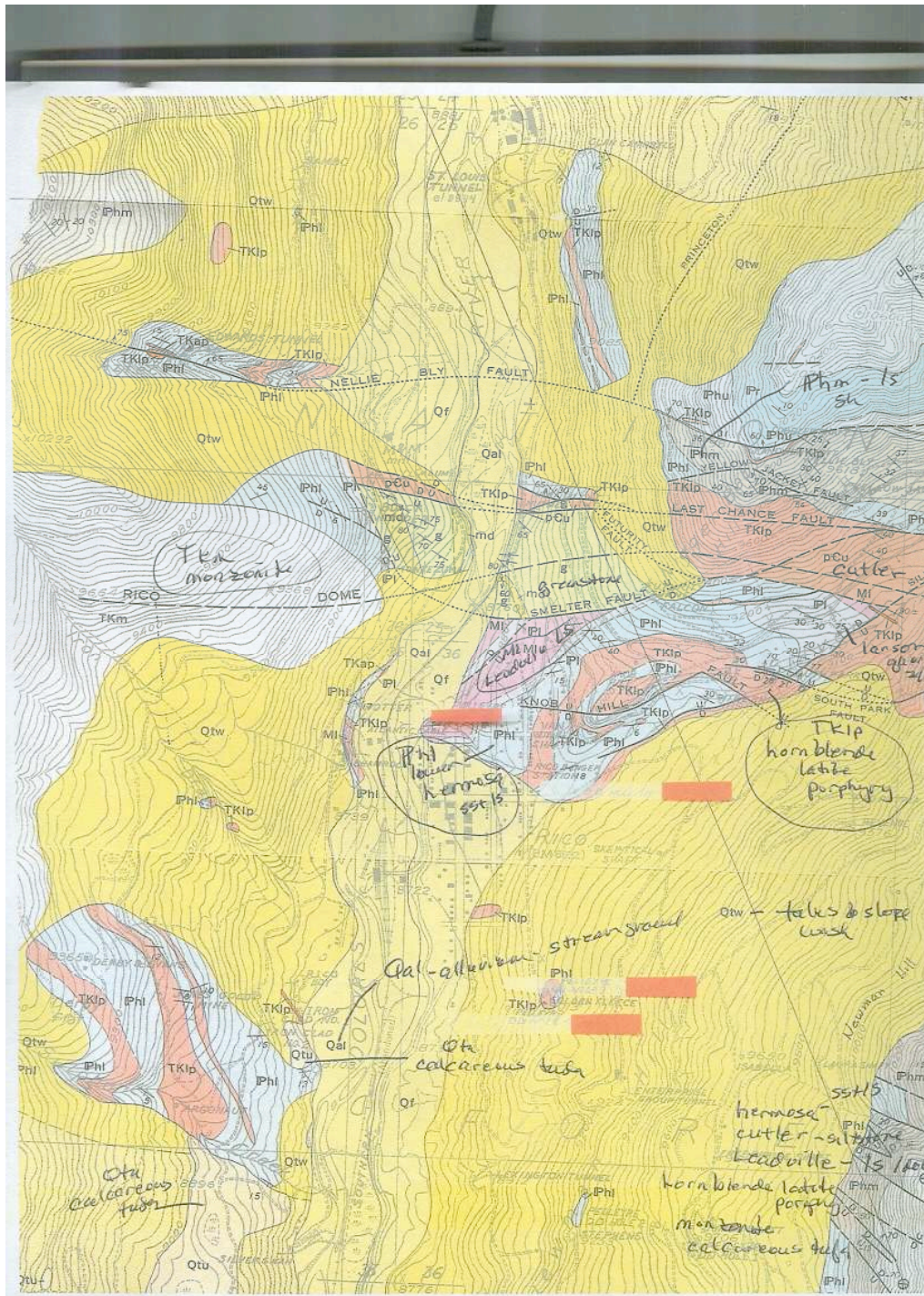
Here we would just like to mention what happens to the pressure equations, when a beam is broken. Because the beams represent the pore walls, and because the fluid is assumed to be incompressible, the pressure within a connected crack has to be constant. In this sense a crack is a macro-pore. Numerically this can break beams very high, i.e.  $k_{ij} = 10^9$ . Hence the pressure drop along a crack is negligibly small.

## 13.0 Appendix B



### Geologic Map of Rico Quadrangle with cross section C-C'(Brown et al, 2009)



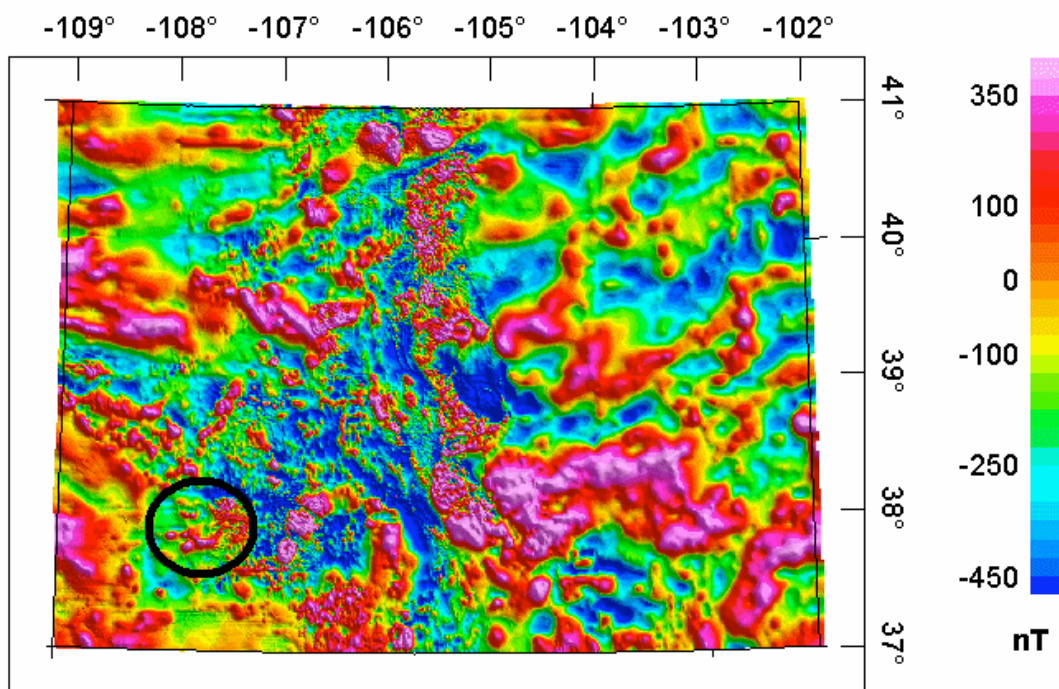


**Geologic Map of Rico showing Leadville Limestone Outcrop illustrated in pink-purple color (Brown et al, 2009)**

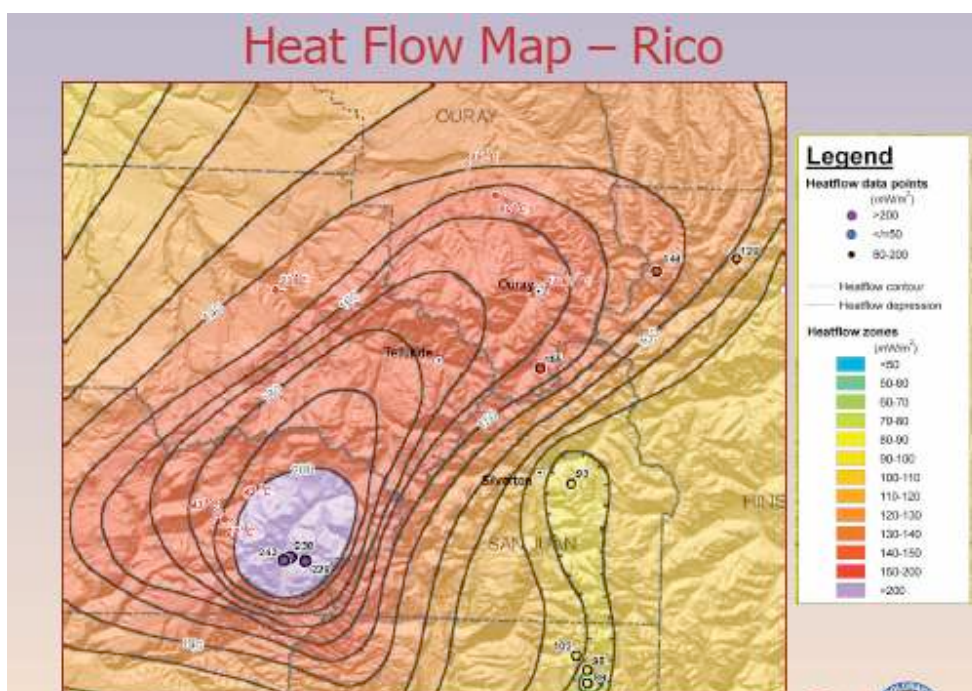
AGE	SW	FORMATION OR GROUP	NE
TERTIARY		San Jose Formation	
		Nacimiento Formation	
		Ojo Alamo Sandstone	
CRETACEOUS	LATE	Kirtland Shale (Farmington Sandstone Member)	1
		Fruitland Formation	1
		Pictured Cliffs Sandstone	1
		Lewis Shale	
		Cliff House Sandstone	1
		Menefee Formation	
		Point Lookout Sandstone	1
		Upper Mancos Shale	1
		Gallup Ss. (Torrivio Mbr.)	1
		Tocito Ss. Lentic	1
		Lower Mancos Shale	
		Greenhorn Limestone	
	EARLY	Dakota Sandstone	
		Burro Canyon Formation	1
JURASSIC		Morrison Formation (Todilto Limestone Member)	
		Wanakah Formation	
		Entrada Sandstone	
TRIASSIC		Chinle Formation	1
PERMIAN	Cutler Group	De Chelley Sandstone	
		Organ Rock Shale	
		Cedar Mesa Formation and related rocks	
		Halgaito Formation	
PENNSYLVANIAN	Hermosa Group	Rico Formation	
		Honaker Trail Formation	
		Paradox Formation and related rocks	1
		Pinkerton Trail Formation	
		Molas Formation	
MISSISSIPPIAN		Leadville Sandstone	
DEVONIAN		Ouray Limestone	
		Elbert Formation	
CAMBRIAN		Ignacio Quartzite	
PRECAMBRIAN			

**Regional Stratigraphy of Paradox Basin(UGS, 2007)**

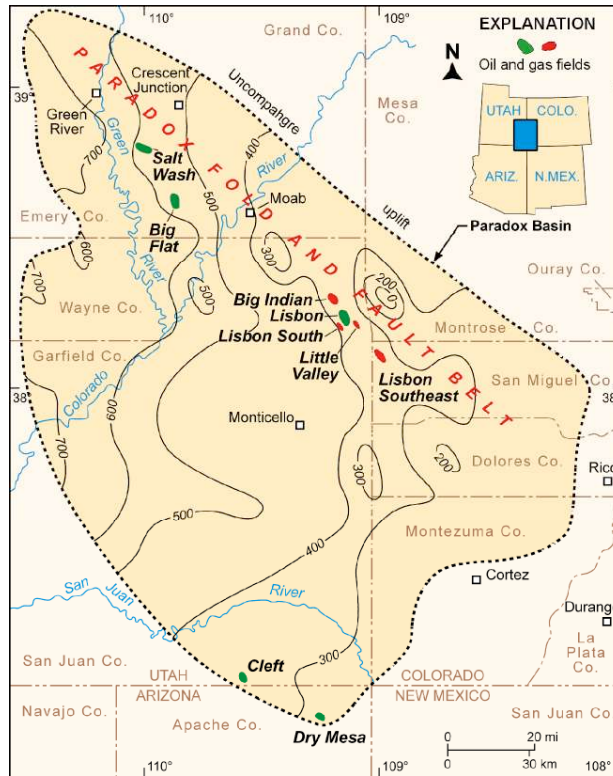




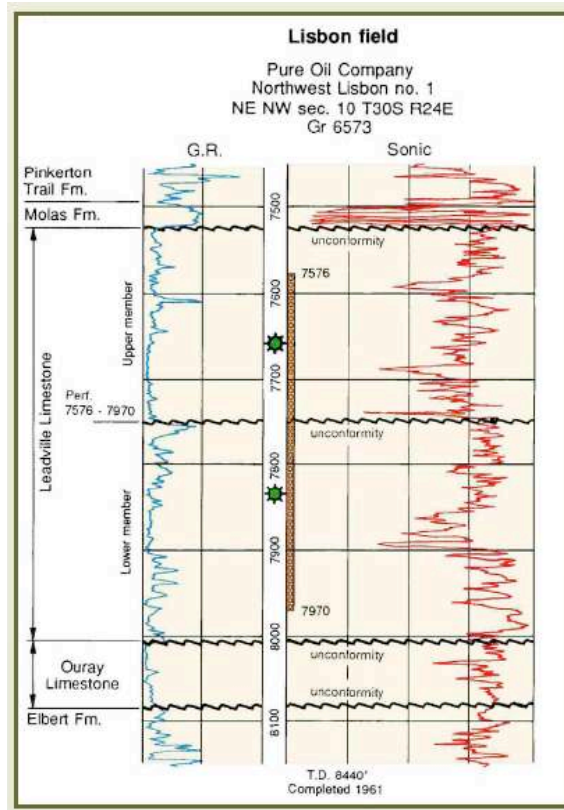
**Regional Magnetic Survey of Colorado (CGS, 2008)**



**Heat Flow Map of Colorado (CGS, 2008)**



**Isopach Map of Leadville Limestone over Paradox Basin (UGS, 2007)**



**Sample Well Log of Leadville Limestone from Lisbon Field (UGS, 2007)**

